

ON THE VIBRATIONAL ENVIRONMENT OF THE "INFLUENCE OF VIBRATIONS ON DIFFUSION OF LIQUIDS" EXPERIMENT

Nuria Sáez¹, Josefina Gavalda², Xavier Ruiz*², Valentina Shevtsova³

¹Departament de Química Física i Inorgànica, Universitat Rovira i Virgili, Tarragona, Spain.
nuria.saez@urv.cat

²Departament de Química Física i Inorgànica, Universitat Rovira i Virgili, Tarragona, Spain.
{josepxavier.ruiz, fina.gavalda}@urv.cat

³Department of Chemical Physics, MRC, Université Libre Bruxelles, Brussels, Belgium.
vshev@ulb.ac.be

Keywords: Accelerometric analyses, Gaussianity, Higher order spectra, Bispectrum, Bicoherence, Trispectrum.

Abstract. *The aim of this work is to study the vibrational impact of the shaker during the past ESA experiment entitled Influence of Vibrations on Diffusion of Liquids, IVIDIL, in the International Space Station, ISS. To do so, we have used accelerometric signals downloaded from the NASA Principal Investigator Microgravity Services, PIMS, website. All signals came from the sensor located in the Columbus module when the shaker is active and correspond to different time periods and different frequencies and amplitudes. With these data we have made a comparative statistical analysis to investigate the propagation of the different frequencies nominally applied to the mechanical shaker as well as the influence of their amplitudes. The consideration of all accelerometric histograms shows that the shaker modifies the normal distribution of the data introducing nonlinearities in the distribution of the energy. Higher Order Statistical techniques allow studying the possible origin of these nonlinearities, in particular, quadratic and cubic frequency couplings phenomena are carefully analysed using the bispectrum, bicoherence and trispectrum functions. Additionally, the analysis of the biphasic and triphasic histograms critically contributes to discern if a quadratic and cubic phase couplings are presents in the signals. These procedures are mandatory in order to clarify the nonlinear transfer mechanism of energy between frequencies.*

1 INTRODUCTION

Digital signal processing is the suitable tool to characterize motorized experiments as the so-called “Influence of Vibrations on Diffusion of Liquids (IVIDIL)” one. First and second order statistics use the mean and variance to characterize the signals in the time domain [1-3]. In frequency, the power spectrum helps to complete the description. But, second order statistical techniques are only sufficient for describing linear processes and a vibrating mechanical system, often shows unstable, non-Gaussian and nonlinear characteristics to some extent, especially when the system become defective. Mechanical failures, if any, are always preceded with changes from linear or weakly nonlinear to strong nonlinear dynamics [4-7], so, it is difficult for conventional analysis based on Fourier transform to find weak fault information. High-order spectral analysis must then be used providing a more effective tool to extract information due to deviations from Gaussianity, to recover the true phase character of the signals and to detect and quantify nonlinearities in the time series.

In previous works we analysed data coming from two accelerometric sensors located in the Columbus and Destiny modules of the International Space Station when the shaking motor of the above-mentioned IVIDIL experiment was active or inactive respectively [8, 9]. Now, in the present work, we focus our attention on a different situation considering data coming only from the same SAMSES ES08 sensor in the Columbus module during active periods of the motor in which the oscillatory movement generated by the shaking motor has different frequencies and amplitudes. In particular, the present signals covers complete experiments – roughly 18 hours– with shaking frequencies of 2 and 2.8 Hz. Amplitudes are, in all cases, between 15 and 62 mm. All accelerometric signals have freely been downloaded thanks to NASA Principal Investigator Microgravity Services, PIMS website as binary files [10]. Notice that the experiment was located into the Glovebox rack (Columbus module), but despite the sensor is situated in the Glovebox, it is not on the experimental device.

So, based on the above-mentioned accelerometric signals and using standard second order and specifically adapted higher order statistical techniques the aim of the present work is to carry out a deep comparative analysis in order to characterize the distortions generated by the activity of the mechanical system, in particular, by the different frequencies and amplitudes of the oscillatory movements applied. To do so we emphasize here on polyspectral techniques, based on the calculation of bispectrum and trispectrum functions. Bispectrum function (third order spectrum) is related with the skewness of the signal and it can detect asymmetric nonlinearities. In the same way, trispectrum magnitude (fourth order spectrum) is sensitive to the signal kurtosis; therefore it can detect symmetric nonlinearities [11]. Bispectrum and trispectrum functions enable to study the Quadratic and the Cubic Phase Coupling phenomena.

Mention also that, because in a Space Station malfunctions are not easy to be removed, the detection and characterization of the impact on the environment is also extremely important. All these results constitute another step towards our final objective, define clearly the global accelerometric environment of the IVIDIL experiment [12].

2 NUMERICAL PROCEDURES

The signals are SAMS data with a sampling rate of 500 Hz, a cut-off frequency of 200 Hz and a gain of 8.5. Data units are in g and in order to eliminate possible instrument bias we have systematically demeaned all the raw signals before attempt any mathematical manipulation. The positions and locations/orientations of the SAMS sensors against the International Space Station Absolute coordinate system (SSA: X_A , Y_A , Z_A) are detailed in the bibliography [13, 14]. It should be pointed out that the results are presented in the X_A direction because is the shaking direction [8].

Frequency domain analyses used the power spectral densities (PSD) estimated by the Welch's method. This method splits the signal into overlapping segments –thirty three in the present case–, calculates the periodogram of each one of them and averages the results to produce the final power spectral density result [3].

If the distribution associated to a signal is not normal, higher order statistical analysis, HOSA, techniques must be used. The Fourier transform of the third order cumulant, called the bispectrum has been estimated as a direct average of the triple products of Fourier transforms over K segments (direct method) [15]. Fourier transforms were calculated considering 2048 FFT points in each one of the 14000 non overlapped segments in which the signal was initially divided. Hamming windows were used in each segment. Important symmetry relations in the frequencies plane (f_1, f_2) results from the definition of discrete bispectrum [16]. In our case we present two regions of symmetry corresponding to positive values of f_1 and f_2 , in which the straight $f_1=f_2$ is the symmetry axis. The bispectrum can be normalized in such a way that it gives a new measure, the bicoherence function. In this work we use the Kim-Powers normalization [17]. The calculation of the bicoherence is a delicate question because the low values of the factors in the denominator could generate a fictitious peak distribution which needs to be carefully corrected using different strategies. In our case we adopted the threshold methodology, that is to say, when the magnitudes that appear in the bicoherence do not overcome a determined threshold, the bicoherence is automatically set to zero. In the present study and after tested different values we finally fixed the thresholds at 1% of the maximum values of these magnitudes [5, 9]. The bicoherence allow us to investigate the existence of quadratic phase coupling. Remember that phase coupling between two frequency components of a signal results in a contribution at a frequency equal to their sum. Additionally, for a quadratic phase coupling the phase of the bispectrum is zero. A previous work [9] has exhibit that a situation of zero biphas it is also equivalent to $\pm\pi$ biphas, because the sampling frequency and the FFT number of points used in the data introduces this indeterminacy in the phase of bispectrum. Here, we use the new biphas histogram method, that is to say, constructing histograms with the values of the biphas of each one of the different segments considered and only at the corresponding frequency couplings. The literature [18] shows that the peaks of bispectrum can be related to the two situations, the first one, a Quadratic phase Coupled phenomenon (QPC), where the components are coupled in frequency and phase, in this case we do not only considerer zero biphas, but also $\pm\pi$. In the second situation the system accomplishes the addition between frequencies but the biphas is constant, that is to say, non-zero. Both situations result of non-zero bispectrum values. Consequently, the study of biphas is critically important to solve if QPC behaviour exists.

The discrete trispectrum also was calculated as an average of the quadruple products of Fourier transform [11, 15]. To ensure statistical confidence for the trispectrum, the segment size to compute the FFT should be the third root of the total data length. To accomplish this, we need a short FFT segment, but in this case, the resolution decrease drastically. We adopted a compromise maintaining the size of segment at 2048 points and an average over 1000 windowed records. The principal domain of the discrete trispectrum is composed of two regions, the first one is defined by positives values of frequencies ($f_1 \geq 0, f_2 \geq 0, f_3 \geq 0$), in which the fourth frequency is equal to the sum of the three frequencies ($f_1+f_2+f_3$). In the second region, defined by ($f_1 \geq 0, f_2 \geq 0, f_3 \leq 0$), the sum of the two frequencies (f_1+f_2) is equal to the sum of the other two. If in both regions the triphase is zero or $\pm\pi$ rad, there is a Cubic Phase Coupling (CPC) phenomenon.

3 RESULTS

Despite the present work involved the analysis of many signals we report four of them, corresponding to the maximum and minimum values of shaking amplitudes for two different frequencies. The first one –thereafter IVIDIL1– correspond to 2.8 Hz of frequency and an amplitude of 31 mm, the second one –called IVIDIL2– coincides with the frequency of IVIDIL1, but in this case has an amplitude of 15 mm. The third signal –IVIDIL3– has a frequency of 2 Hz and its amplitude is 62 mm, and finally, the last signal presented – IVIDIL4– corresponds to the same frequency of IVIDIL3 although its amplitude is 31 mm.

Figure 1, the ten second interval average, is a representative plot of the entire signals analysed (X_A axis acceleration), where we can see as the mean is approximately the same in all cases. Also, we have to mention that in Y_A and Z_A axes we have found a fluctuation with a period of 90 minutes (the orbital period).

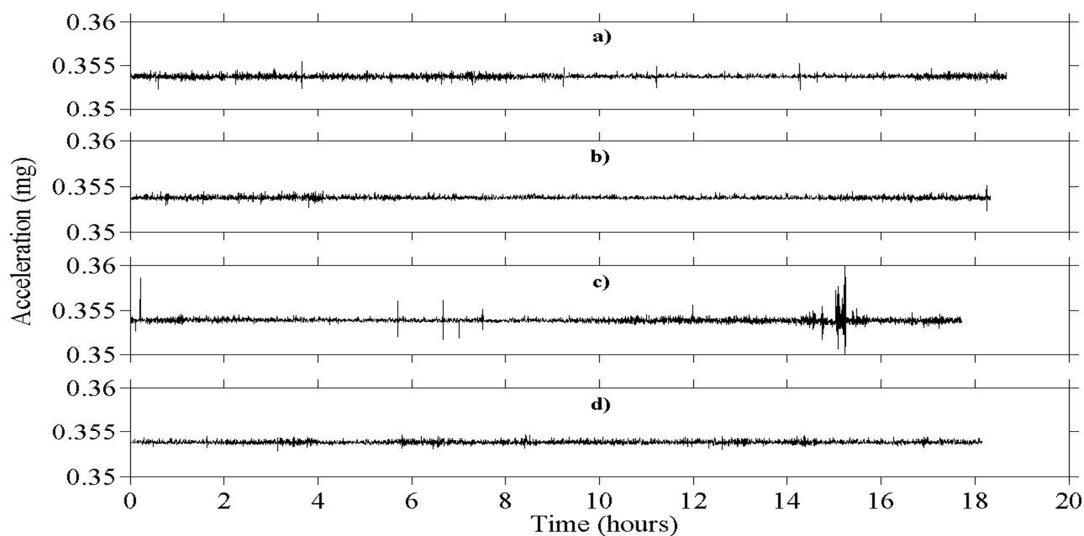


Figure 1: 10s interval average of X_A axis acceleration: a) IVIDIL1, b) IVIDIL2, c) IVIDIL3 and d) IVIDIL4.

In order to check the differences between the means and obtain additional statistical information, we present Table 1, where we can observe that the percentage of outliers is very low, although, the couples as 2.8 Hz as 2 Hz show the higher value in the maximum amplitude signal (IVIDIL1 and IVIDIL3). Also, the table shows the values of the interquartile range, IQR [19], indicating the dispersion of the data.

Signals	Mean (mg)	Median (mg)	IQR (mg)	Outliers (%)
IVIDIL1	0.3537	0.3524	0.3422	$5.5 \cdot 10^0$
IVIDIL2	0.3538	0.3540	0.5152	$2.4 \cdot 10^{-3}$
IVIDIL3	0.3539	0.3519	0.6577	$4.5 \cdot 10^{-3}$
IVIDIL4	0.3538	0.3642	0.3908	$1.2 \cdot 10^{-4}$

Table 1: Basic descriptive statistics of the four signals.

Figure 2 shows the above-mentioned dispersion and also the clear multimodal behaviour, that is to say, a non-Gaussian distribution. The same happens with all X_A axis acceleration data analysed even though they are not displayed here. We have also proved in the Y_A and Z_A axes but they have a normal tendency.

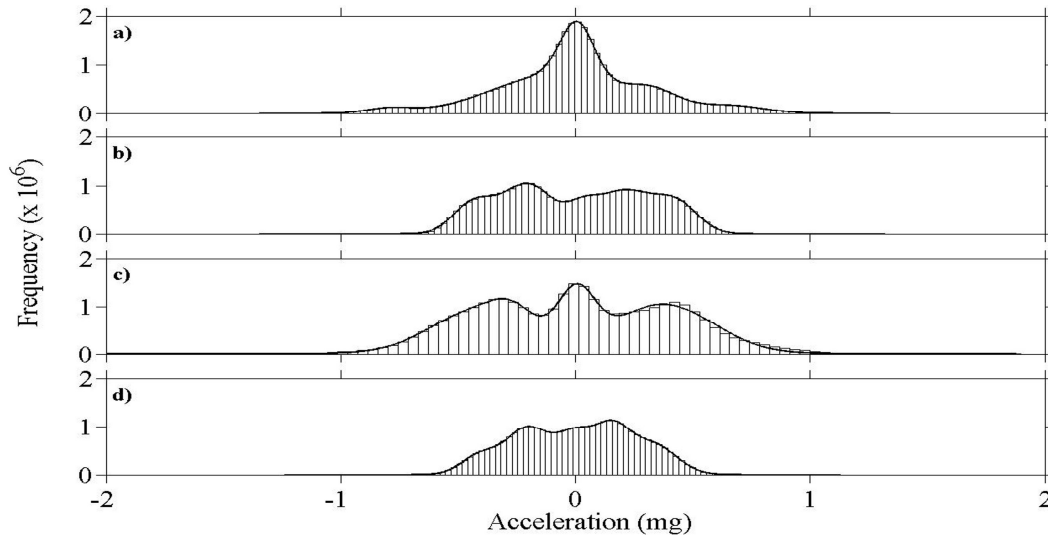


Figure 2: Histograms of X_A : a) IVIDIL1, b) IVIDIL2, c) IVIDIL3 and d) IVIDIL4.

To study the influence of the shaking amplitudes, Figure 3 presents the power spectra and its quantitative results in Table 2. This analysis indicates that the amplitudes change the intensity of the harmonics in signals of the same frequency and that the most energetic frequencies are in the signals of maximum amplitudes. Furthermore, we can see that the third harmonic, $3f_0$ (8.4 Hz for 'a)' and 'b)' and 6 Hz for 'c)' and 'd)' cases), is higher than the fundamental frequency, f_0 , in all cases. It maybe due to nonlinear phenomena generated by some kind of mechanical malfunction or for the location of the sensor far away of the experiment.

Frequency (Hz)	Intensity (g^2/Hz)			
	IVIDIL1	IVIDIL2	IVIDIL3	IVIDIL4
2	-	-	$2.15 \cdot 10^{-4}$	$4.17 \cdot 10^{-5}$
2.8	$1.75 \cdot 10^{-3}$	$1.91 \cdot 10^{-4}$	-	-
4	-	-	$5.60 \cdot 10^{-6}$	$8.97 \cdot 10^{-9}$
5.6	$1.40 \cdot 10^{-6}$	$2.73 \cdot 10^{-8}$	-	-
6	-	-	$3.50 \cdot 10^{-3}$	$7.80 \cdot 10^{-4}$
8	-	-	$1.50 \cdot 10^{-5}$	$1.67 \cdot 10^{-5}$
8.4	$2.76 \cdot 10^{-3}$	$2.97 \cdot 10^{-3}$	-	-
10	-	-	$2.90 \cdot 10^{-4}$	$3.06 \cdot 10^{-4}$
11.2	$1.31 \cdot 10^{-6}$	$2.62 \cdot 10^{-6}$	-	-
12	-	-	$7.89 \cdot 10^{-8}$	$3.56 \cdot 10^{-6}$
14	$1.10 \cdot 10^{-4}$	$1.28 \cdot 10^{-4}$	$2.04 \cdot 10^{-5}$	$2.53 \cdot 10^{-4}$
18	-	-	$2.22 \cdot 10^{-5}$	$4.51 \cdot 10^{-6}$
19.6	$2.07 \cdot 10^{-4}$	$2.52 \cdot 10^{-6}$	-	-
22	-	-	$7.76 \cdot 10^{-6}$	$2.91 \cdot 10^{-6}$
25.2	$1.59 \cdot 10^{-5}$	$1.85 \cdot 10^{-5}$	-	-
26	-	-	$1.21 \cdot 10^{-5}$	$3.03 \cdot 10^{-5}$
73.1	$4.06 \cdot 10^{-6}$	$4.06 \cdot 10^{-6}$	$3.20 \cdot 10^{-6}$	$3.74 \cdot 10^{-6}$

Table 2: Frequencies and intensities from Power Spectral Density.

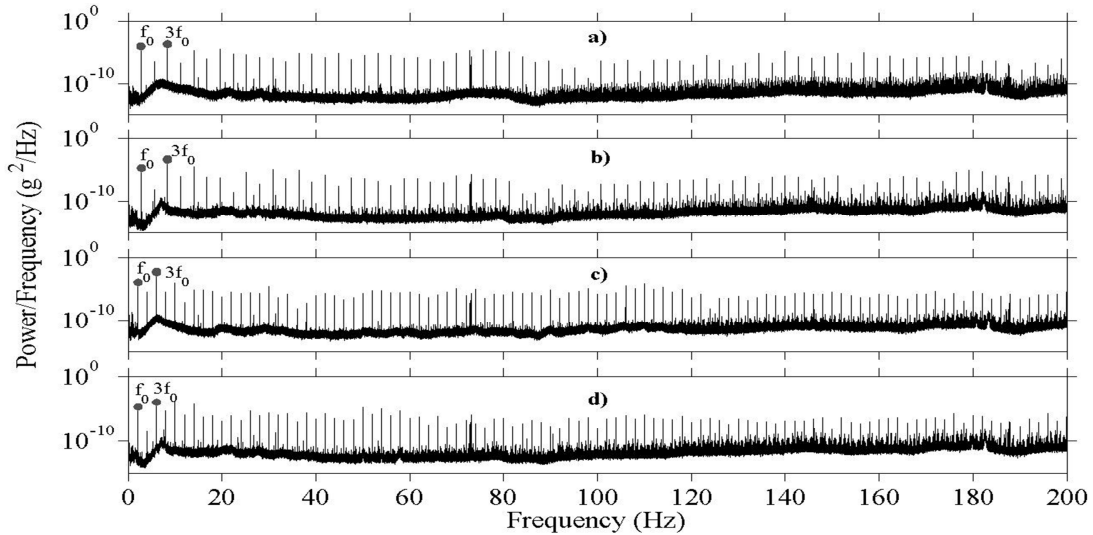


Figure 3: PSD (Welch method) of X_A acceleration: a) IVIDIL1, b) IVIDIL2, c) IVIDIL3 and d) IVIDIL4.

Figure 4 shows the bispectrum contour for the four signals analysed. We can see that different behaviours are presented depending on the shaking frequency. In the case of IVIDIL1 and IVIDIL2 (2.8 Hz), the bispectrum maximum values are located always in the same (8.4,8.4) couple, while for the cases IVIDIL3 and IVIDIL4 (2 Hz) the maximum bispectrum values change depending on the amplitude of the oscillatory force. In this case, for low amplitudes the maximum bispectrum values are associated to (6,6) and (8,6) couples, while at high amplitudes the maximum bispectrum values are associated to (6,4) and (10,6) pairs.

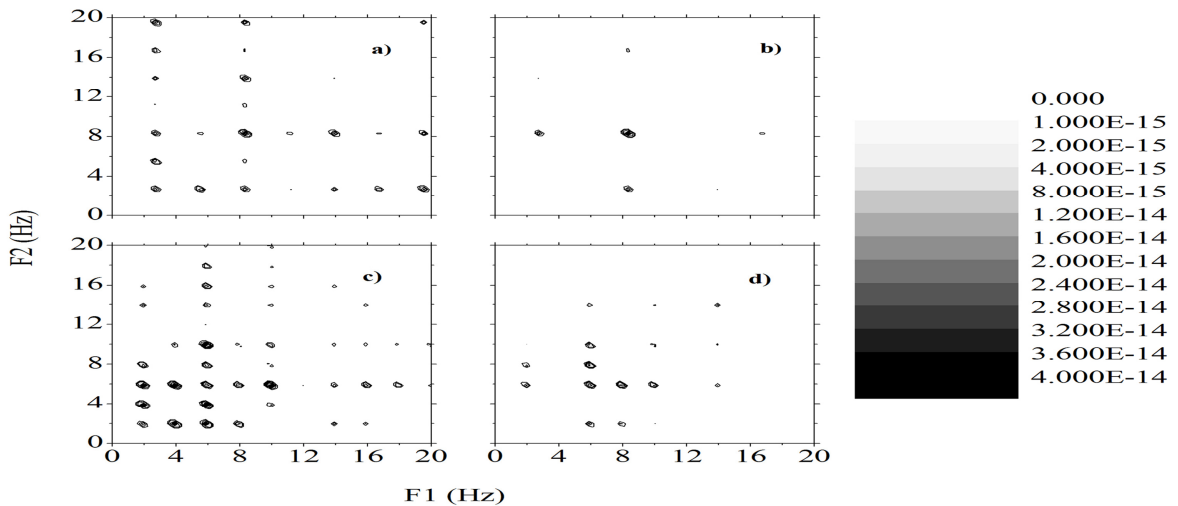


Figure 4: Bispectrum: a) IVIDIL1, b) IVIDIL2, c) IVIDIL3 and d) IVIDIL4.

Figure 5 presents typical biphas histograms found in the different accelerometric signals associated to the bispectrum peaks. The cases 'a)' and 'd)' correspond to a QPC situation, the biphas is distributed around zero (case 'a)') or $\pm\pi$ (case 'd)'). A partial QPC phenomenon (PQPC) is exhibited in case 'b)' and 'e)', where it appears different distributions in zero, $\pm\pi$ and also other angular positions. Then, we can calculate the percentage of coupling associated to a particular case in the histograms, taking into account the surface relation between (0, $\pm\pi$) and the constant phases. Statistical criterions [20] allow to fix the acceptance phase region

around the peaks of the biphas (in our case, the value of the acceptance region is of ± 0.1 rad) [21]. Finally, a constant biphas situation (CP) is presented in the cases 'c)' and 'f)'.

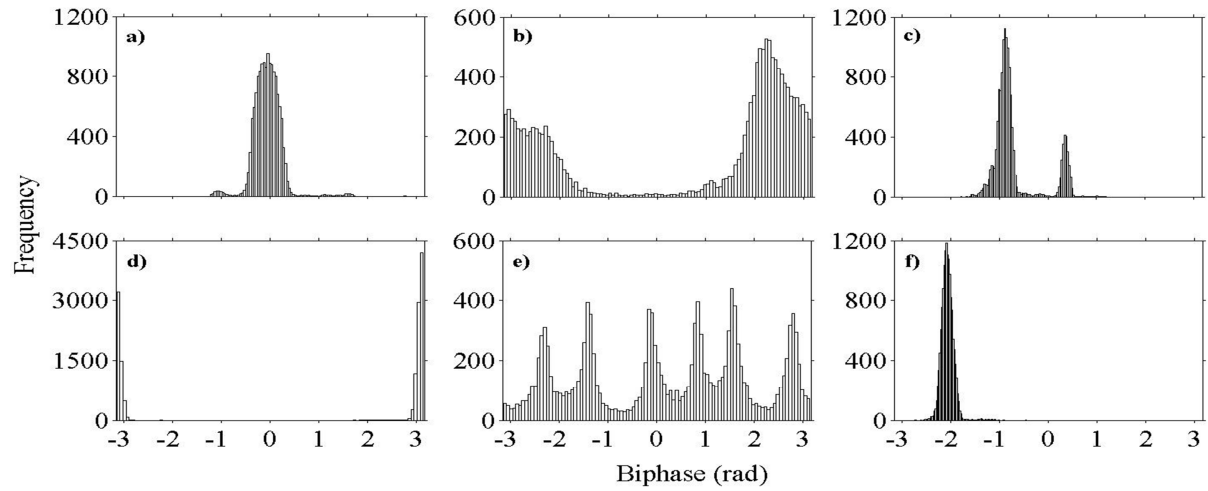


Figure 5: Typical biphas histograms. a)QPC, b)PQPC, c)CP, d)QPC, e)PQPC and f)CP.

Couples	2 Hz & Amplitude (mm)			2.8 Hz & Amplitude (mm)		
	31	52	62	15	23	31
(2.8,2.8)	-	-	-	PQPC(24%) 0.34 [0.08]	PQPC(24%) 0.84 [0.2]	PQPC(13%) 0.47 [0.06]
(4,2)	PQPC(17%) 0.60 [0.10]	CP(0.3rad)	CP(0.37rad)	-	-	-
(5.6,2.8)	-	-	-	PQPC(33%) 0.34 [0.11]	CP(-2.16rad)	PQPC(16%) 0.59 [0.09]
(6,4)	PQPC(26%) 0.61 [0.16]	CP(1.6rad)	CP(2.9rad)	-	-	-
(8.4,2.8)	-	-	-	CP(-0.91rad)	CP(-1.92rad)	QPC(0rad) 0.78
(6,6)	CP(-1.8rad)	CP(-2.34rad)	CP(2.67rad)	-	-	-
(8.4,5.6)	-	-	-	PQPC(16%) 0.34 [0.05]	PQPC(51%) 0.84 [0.42]	PQPC(12%) 0.63 [0.08]
(8,6)	CP(-0.82rad)	PQPC(15%) 0.69 [0.10]	CP(2.19rad)	-	-	-
(8.4,8.4)	-	-	-	CP(-2.73rad)	CP(-0.35rad)	CP(-2.07rad)

Table 3: Biphas and bicoherence results.

Table 3 summarizes these results for the principal pairs of the bispectrum. The first line presents the corresponding situation (QPC, PQPC or CP), between parenthesis it gives the angular biphas values (CP cases) or the percentage of coupling for PQPC cases. The second line (in bold) shows the bicoherence values only in the cases of QPC and PQPC. Previous work [9] point that, in the case of PQPC behaviour, the bicoherence magnitude is due to both (QPC and CP) contributions, thus, taking into account the percentage of PQPC calculated, we correct the bicoherence values. These results are presented in brackets. We are interested in

some couples that could explain the higher values of power spectrum of third harmonic (8.4 and 6 Hz). From Table 3, we can see that only the couple (2.8,2.8) exhibits a PQPC behaviour, the couple (2.8,5.6) not always presents a PQPC. In the case of IVIDIL3 and IVIDIL4 even it is more difficult associate a PQPC phenomenon. Thus, a quadratic nonlinear contribution seems to be not relevant enough to explain this behaviour.

To go further, we analysed the trispectrum function, which is displayed in Fig. 6 for IVIDIL1 and IVIDIL3 signals by drawing spheres and the corresponding projections in the trifrequency space. The size of the spheres is proportional to the square root of the trispectrum magnitude. The centres of the biggest spheres appearing in Figure 6 are also checked by the triphase histogram. As an example, Fig.7 shows the triphase histograms associated to the maximum values of trispectrum (8.4,8.4,-8.4) and (6,6,-6) for IVIDIL1 and IVIDIL3 respectively. The points (8.4,2.8,-2.8), (8.4,8.4,-8.4) and (6,6,-6), (6,2,-2) present frequency and phase coupling, this could explain the higher power spectral intensities of the third harmonic. Additionally the high values of $5f_0$ frequency can be produced by the CPC at the coupled frequencies (14,8.4,-8.4) and (10,6,-6). It seems that cubic symmetric nonlinearities are mainly responsible of the mechanical system behaviour.

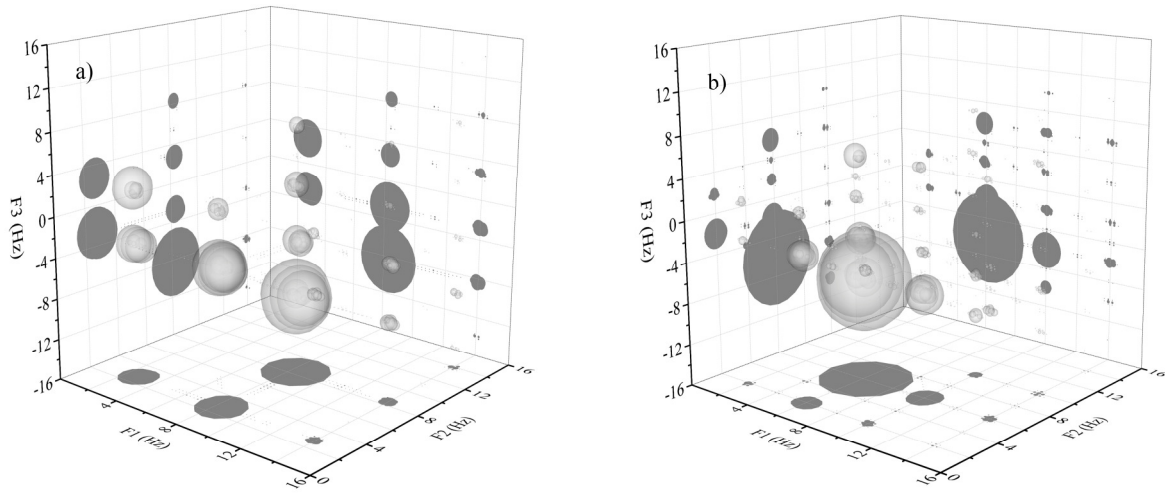


Figure 6: Trispectrum: a) IVIDIL1 and b) IVIDIL3.

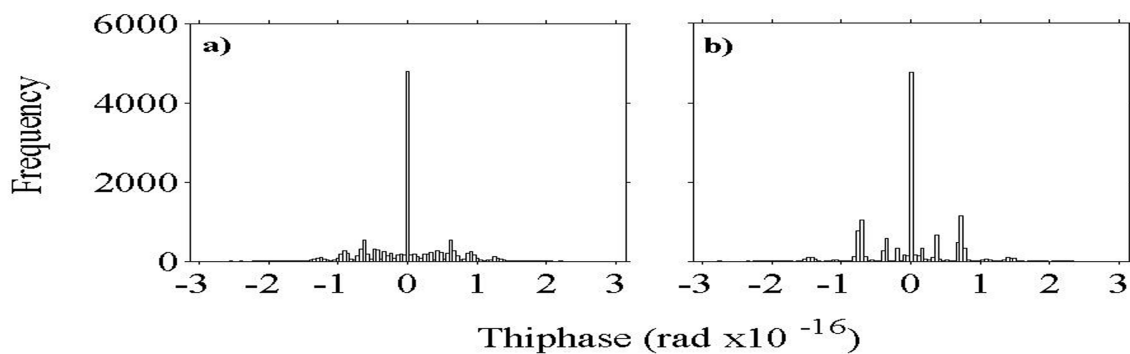


Figure 7: Triphase: a) IVIDIL1(8.4,8.4,-8.4) and b) IVIDIL3 (6,6,-6).

4 CONCLUSIONS

- Power spectral analysis determines that the third harmonics have bigger power spectral magnitude than the fundamental one. If the amplitude of vibrating force increases, usually increases the power spectra intensities.
- Bispectrum maximum values are always observed at the same peaks for IVIDIL1 and IVIDIL2 signals, while there are a change the positions for IVIDIL3 and IVIDIL4 signals. It seems that the influence of the amplitude is more relevant in the case of signals with 2Hz fundamental frequency.
- Biphase histograms analysis introduces primordial information discarding the couples that, even frequency coupled, do not present QPC phenomenon. In general, we found that no relevant QPC behaviour exists.
- Cubic Phase Coupling phenomenon is clearly observed in the signals. It is responsible of the high power spectra intensities associated to a third harmonic and even the fifth one, Triphase histograms corroborate this behaviour. The high magnitude of the third harmonic maybe due to symmetric nonlinearities present in the motorized mechanical equipment –Cubic Phase Coupling phenomenon– or perhaps any kind of unknown external contamination due to the localization of the sensor, not on the experiment.

ACKNOWLEDGMENTS

The content of the present work is part of our participation in the HSF-US/2010-042 and HSF-US/2010-041 ESA projects.

REFERENCES

- [1] K. Hrovat, PIMS Real-Time Data Reception and Environment Characterization. *19th International Microgravity Measurements Group Meeting*; Glenn Research Center, Cleveland, Ohio 2000.
- [2] K. Hrovat, Analysis Techniques for vibratory data. *NASA 7th Annual Microgravity Environment Interpretation Tutorial*, NASA Glenn Research Center, Ohio Aerospace Institute, Cleveland, Ohio 2004.
- [3] M.J.B. Rogers, K. Hrovat, K. McPherson, M.E. Moskowitz and T. Reckart, *Accelerometer Data Analysis and Presentation Techniques*. NASA Lewis Research Center, Cleveland, Ohio, 1997.
- [4] Y. Jiangtian, Z. Lihua, C. Jiaji and Z Ziping, Higher order spectra and its application in machinery fault diagnosis. *Transactions of Tianjin University*, **5**, 190–194, 1999.
- [5] N. Jaksic, M. Boltezar, I. Simonovski and A. Kuhelj, Dynamical behaviour of the planar nonlinear mechanical system - Part I: Theoretical Modelling. *Journal of Sound and Vibrations*, **226(5)**, 923–940, 1999.
- [6] M. Boltezar, N. Jaksic, I. Simonovski and A. Kuhelj, Dynamical behaviour of the planar nonlinear mechanical system - Part II: Experiment. *Journal of Sound and Vibrations*, **226(5)**, 941–953, 1999.

- [7] Jyoti K. Sinha, Higher Order Coherences for Fatigue Crack Detection, *Engineering Structures*, **31**, 534–538, 2009.
- [8] N. Sáez, X. Ruiz, Jna. Gavalda, J. Pallarés and V. Shevtsova, Comparative ISS Accelerometric Analyses. *Acta Astronautica*, 2013 (Submitted).
- [9] N. Sáez, X. Ruiz and Jna. Gavalda A comparison between different accelerometric signals in two different modules of the International Space Station. *Aerospace Sciences and Technology*, 2013 (Submitted).
- [10] <http://pims.grc.nasa.gov/html/ISSAccelerationArchive.html>.
- [11] W. B. Collis, P. R. White and J. K. Hammond, Higher-order spectra: the bispectrum and trispectrum, *Mechanical Systems and Signal Processing*, **12(3)**, 375–394, 1998.
- [12] N. Sáez, X. Ruiz, J. Pallarés, V. Shevtsova, On the accuracy of the interdiffusion coefficient measurements of high temperature binary mixtures under ISS conditions, *Comptes Rendus Mecanique*, **341(4–5)**, 405 – 416, 2012.
- [13] Principal Investigator Microgravity Services, *International Space Station, PIMS Acceleration Data File Description Document*. NASA Gleen Research Center, Ohio, PIMS-ISS-101, 2002.
- [14] K. Jules, K. Hrovat, E. Kelly and T. Reckart, *International Space Station Increment 6/8. Microgravity Environment Summary Report*, NASA/TM-2006-213896, 2006.
- [15] A. Rivola, Applications of higher order spectra to the machine condition monitoring. *Publ. DIEM, University of Bologna*, **107**, 2000.
- [16] V. Chandran and S. Elgar, A General Procedure for the Derivation of Principal Domains of Higher-Order Spectra. *IEE Transactions on signal processing*, **42(1)**, 229–233, 1994.
- [17] Y.C. Kim and E.J. Powers, Digital bispectral analysis and its applications to nonlinear wave interactions. *IEEE Transactions on Plasma Science*, **7(2)**, 120–131, 1979.
- [18] D. Wong, D.A. Clifton, L. Tarassenko, An introduction to the bispectrum for EEG analysis. *5th Conference in Biomedical Engineering and Medical Physics*, PGBIOMED, United Kingdom, 61–62, 2009.
- [19] R. McGill, J.W. Tukey and W.A. Larsen, Variation of Boxplots. *The American Statistician*, **32(1)**, 12–16, 1978.
- [20] S. Elgar and G. Sebert, Statistics of bicoherence and biphas. *Journal of Geophysical Research*, **94(8)**, 993–998, 1989.
- [21] J.W.A. Fackerell, Bispectral analysis of speech signals. *Doctoral Thesis*, University of Edinburg, 1996.